THE JOURNAL OF PHYSICAL CHEMISTRY B

Article

pubs.acs.org/JPCB

Car−Parrinello Molecular Dynamics/Molecular Mechanics (CPMD/MM) Simulation Study of Coupling and Uncoupling Mechanisms of Cytochrome P450cam

Peng Lian,[†] Jue Li,[†] Dong-Qi Wang,*[,‡] and Dong-Qing Wei*[,†]

[†]State Key Laboratory of Microbial Metabolism, and College of Life Science and Biotechnology, Shanghai Jiao Tong University, Shanghai, China 200240

[‡]Laboratory of Physical Chemistry, Swiss Federal Institute of Technology, ETH, CH-8093 Zurich, Switzerland

Supporting Information

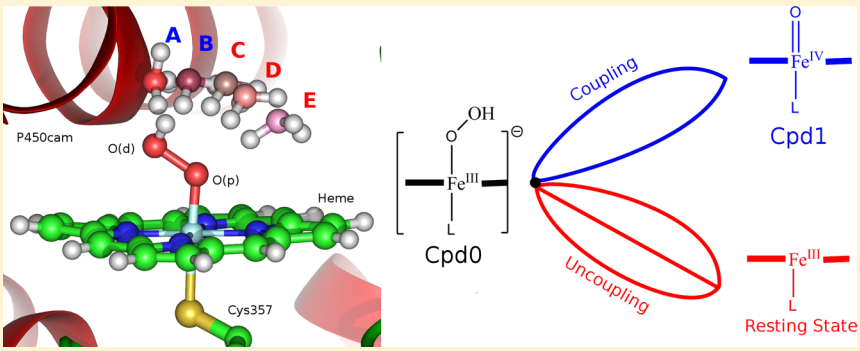

ABSTRACT: The relevance of the pathway through which the second proton is delivered to the active site of P450cam and the subsequent coupling/uncoupling reactions has been investigated using Car−Parrinello molecular dynamics/molecular mechanics (CPMD/MM) dynamics simulations. Five models have been prepared, representing delivery pathways in the wild-type enzyme and its mutants in which Thr252 mutated into other residues with different side-chain length and hydrophobicity. In the simulations, coupling reaction is observed in the wild-type enzyme (Model A) and its T252S mutant (Model B), while the uncoupling products are obtained in the other three models (C, D, and E). Different from previous studies, a dynamic process of the last stage of coupling/uncoupling was observed. We found that the peroxide bond cleavage in coupling, the Fe−O bond stretching in uncoupling, proton transfer, and electron delivery take place spontaneously. Moreover, besides the intrinsic chemical differences between the two peroxide oxygen atoms, water molecules in the active site and the proton transfer pathway may play an important role in the determination of coupling/uncoupling. We conclude that by maintaining a specific proton transfer channel, Asp251−Thr252 channel, the wild-type enzyme could efficiently deliver the second proton to the ideal position for coupling reaction.

INTRODUCTION

Cytochrome P450 is a superfamily of mono-oxygenases with an immense biological impact of drug metabolism.[1] It catalyzes various stereospecific and regioselective processes of oxygenation of the substrates[2−5] through two reducing equivalents.[1] A broad interest on the catalytic mechanism of P450 has been seen among researchers in chemistry, biology, and other relevant fields since decades ago, and a consensus catalytic cycle has been proposed as in Figure 1.[5−10] There are two protonation steps in this cycle. One is the protonation of the ferric peroxo (or ferric superoxo, **S5**) species, which gives the ferric hydroperoxo complex (Compound 0, Cpd 0). The other one is the subsequent proton transfer that produces the iron(IV) oxo porphyrin π-cation radical intermediate (Compound I, Cpd I), which has been proposed to be the active species in the catalysis of P450 by experimental[10−13] and computational[14,15] studies. Cpd 0 is believed to be a precursor of Cpd I; however, it was not well characterized until Naruta and co-workers synthesized the similar ferric hydroperoxo porphyrin complex successfully.[16] Cpd 0 was ever proposed as the "second oxidant" of P450 based on the findings that site-specific mutant of P450, which supposedly blocked the second proton transfer still shows significant activity in substrate oxygenation.[17,18] However, a series of experimental and computational studies[6,19−22] show that Cpd I is an oxidant superior over Cpd 0. Thus the second proton transfer, which relates to the generation of Cpd I from Cpd 0, is of more interest.[8,19,23−31]

The second proton transfer may lead to either the coupling process or the uncoupling one. In the coupling process, the

Received: December 9, 2012
Revised: June 4, 2013

   dx.doi.org/10.1021/jp312107r | J. Phys. Chem. B XXXX, XXX, XXX−XXX

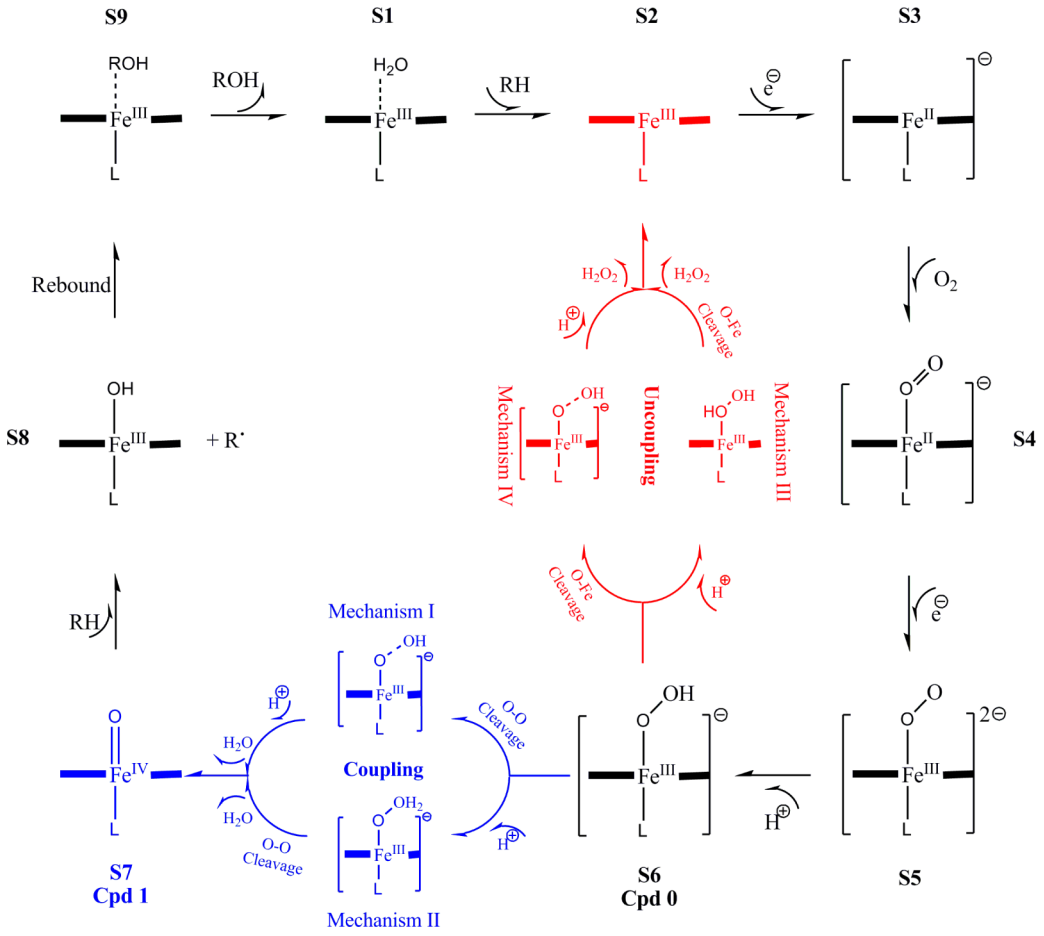

Figure 1. The catalytic cycle of P450. Possible mechanisms[25] for coupling and uncoupling reactions are shown in blue and red, respectively.

proton is transferred to the distal oxygen [the terminal O atom of the FeOO moiety, denoted as O(d); see also Figure 2] of Cpd 0, then the O−O bond is cleaved and Cpd I is generated. In the uncoupling process, a hydrogen peroxide is produced, and the enzyme goes back to its resting state after the proximal oxygen [the bridging O atom in the FeOO moiety, denoted as O(p)] of Cpd 0 received the proton. These two reactions compete against each other and affect the overall turnover rate of the catalysis of substrates. However, the factors that determine the fate of Cpd 0 during the second protonation of the catalytic cycle of P450 remain to be clarified.

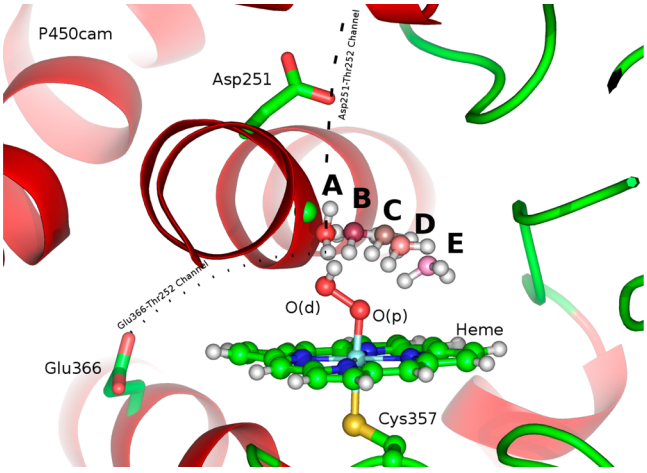

Figure 2. Superposition of the five models A−E. These models are different in the position of the hydronium probe (H_3O^+). The prophyrin, the hydroperoxo moiety, and the hydronium probe are represented in ball-and-stick. The P450cam enzyme is shown in carton. The Asp251-Thr252 channel (dash line) and the Glu366-Thr252 channel (dot line) are shown schematically.

Proton transfer channels seem to play a role in the determination of coupling/uncoupling. Two main channels in P450cam were found: Glu366-Thr252 and Asp251-Thr252.[5,23,25,26,32,33] The Glu366-Thr252 channel is able to provide a proton to the active site via the Poulos−Kraut mechanism.[10,24] However, without direct connection to bulk water, Glu366 is difficult to get reprotonated after offering its proton; therefore, it is questionable on how the deprotonated Glu366 to be replenished to its protonated state. In contrast, the Asp251-Thr252 channel extends the active site to the bulk solvent and shuttles the proton transfer via the Asp251-Arg186 salt bridge.[10,24] In addition, an energy barrier of 6.6 kcal/mol to the proton transfer in the Glu366-Thr252 channel is expected, while it is essentially barrierless in the Asp251-Thr252 channel.[24] Thus, in this study, we consider the Asp251-Thr252 channel.

The importance of Asp251 has been stressed in previous mutagenesis studies.[10,23,28,31] The oxygen-consuming rate and coupling/uncoupling productions have been measured for the wild-type P450cam and its mutants (see Table S1). These observations show that mutations on Asp251 reduce the catalytic rate greatly, while having little effect on the product formation. This could be explained by the solvent accessibility

dx.doi.org/10.1021/jp312107r | J. Phys. Chem. B XXXX, XXX, XXX−XXX

of Asp251, which controls the proton shuttle through a "carboxylate switch" mechanism.[10,33] However, mutations on Thr252 exhibit interesting differences.[25] If it was a residue with hydrophilic and medium-sized side-chain, like Thr and Ser, the coupling product, 5-exohydroxycamphor could be produced quickly. Otherwise, if it was replaced by an amino acid with hydrophobic and large side-chain, like Val and Ile, both the reaction rate and the ratio of coupling product would decrease greatly. For mutants with a short side-chain, like Ala and Gly, uncoupling could be observed. It seems the subsequent effect of the Thr252 mutations depends on the hydrophobicity and the volume of its side-chain.

Recently, theoretical studies[25,26] on P450cam at the quantum mechanics/molecular mechanics (QM/MM) level have shown how proton transfer pathways are constructed by key residues and water molecules may be responsible for the competition between coupling and uncoupling. Several possible pathways, e.g., Asp251-Wat901-Thr252-FeOOH, Asp251-Wat901-FeOOH, and Asp251-Wat901-WatS-FeOOH, were explored in these studies. It has been found that with an extra water molecule (WatS), the uncoupling barriers was reduced from 23 to 29 kcal/mol to 19, 12, and 12 kcal/mol for T252V, T252A, and T252G, respectively. This suggests water molecules inside the active site play an important role in promoting the uncoupling reaction in the mutants. In addition, as it is known, the proton could be transferred freely between water molecules via Grotthuss mechanism (the barrier is around 2−3 kcal/mol[34]). Therefore, there may be multiple options for the enzyme to choose different proton transfer pathways for delivering a proton to the hydroperoxo unit. Thus, one may argue that the observed coupling/uncoupling in Thr252 mutants may be due to the change of the proton-transfer pathways.

In this article, the relationship between proton-transfer pathways and the competition of coupling/uncoupling was studied by Car−Parrinello molecular dynamics/molecular mechanics (CPMD/MM) dynamics simulations. Five models, A−E, were prepared to explore the possible pathways of the second proton transfer step in the P450 cycle of different Thr252 mutants.

METHODS

Set-Up of Systems. A crystal structure[10] (PDB Code: 1DZ8) was used as the initial coordinates. The protocols developed by Thiel's group[25,35−38] were employed for protonation and solvation procedures. The T252G mutant was introduced. This mutation provides enough space in the active site for studying possible proton transfer pathways in all other mutants as well as the wild-type enzyme. Moreover, it causes little conformation changes to the active site according to the following calculations. The substrate camphor was removed to make sure the intrinsic proton affinities of O(p) and O(d) are investigated. Then the geometry of the HOO moiety, heme unit, and the axial Cys ligand were optimized in the gas phase using the deMon package.[39] After that, an energy minimization was performed on the whole system including the enzyme and 6156 solvent water molecules (SPC model was used for water).[40] During the minimization the heme unit, the sulfur and the C_β of Cys357 were fixed. The OPLS all-atoms force field and GROMACS package were used.

The optimized system was then used to load the hydronium probe (H_3O^+). Five models (A−E) shown in Figure 2 were built. Model A was constructed to mimic the wild-type enzyme. In this model, both the oxygen atom [O(aq)] and the to-be-transferred proton [H^+(aq)] of the probe were kept at the same positions as those in the hydroxyl group of Thr252 in the previous study of Wang et al.[38] The other two protons of the probe were optimized accordingly. B and D were built to simulate cases in the T252S and T252V mutants, respectively.[25] Model C served as a reference for coupling and uncoupling. In Model C, both O(aq) and H^+(aq) of the probe were placed equidistantly to O(d) and O(p). Meanwhile, those four atoms [O(aq), H^+(aq) from the probe, O(d) and O(p) of the hydroperoxo unit] were kept on the same plane with H^+(aq) closer to the peroxide group. The other two protons of the probe were balanced symmetrically according to the orientation of the peroxide bond and the O(aq)−H^+(aq) bond of the probe. E represented Oprea et al.'s two-state mode water channel.[41] Different from the other residue−water channels mentioned above, this channel is made up by waters and starting from the Cys ligand side of the porphyrin ring. It is considered as another possible pathway for connecting the active site to the enzyme surface.

QM/MM Calculations. Each model was dealt with the same procedure below. The hydronium probe, the heme unit, and the side chain of Cys357 (49 atoms in total) were defined as QM region and calculated by CPMD program (http://www.cpmd.org/). For QM calculations, with the consideration of both the accuracy and the computing resources the GGA DFT method BLYP[42] was used. The potential between ionic cores and valence electrons was described by Vanderbilt ultrasoft pseudopotentials (USPPs).[43−45] The cutoff of the wave function was set to 25.0 Ry. The rest of each system, including the P450cam enzyme, the waters and the ions was the MM part, and was described by the OPLS all-atom force field[46,47] as implemented in GROMACS.[48−50] For the MM part, in order to avoid nonphysical polarization, atoms within 15 Å of the QM region and all the polar residues as well as ions in the system were chosen as the inner layer. The polarization effect of the inner layer was taken into account by the s-wave partial wave expansion method which was provided by the GROMACS-CPMD QMMM interface.[51] The boundary of QM/MM was treated by the hydrogen link atoms model.[52]

QM/MM geometry optimization was carried out by using the preconditioned conjugate gradients method.[53] The criterion for the convergence of geometry was 5×10^{-3} Å. During the geometry optimization, the coordinates of O(aq) and H^+(aq) of the probe, O(d) and O(p) in the hydroperoxo moiety, the iron, the sulfur and the C_β atom of Cys357 were fixed. The MM part was equilibrated to 300 K in 5 ps using the Berendsen algorithm[54] with the QM region fixed. After that, the QM/MM *ab initio* MD was performed. For the QM region, the Car−Parrinello molecular dynamics[55] with a time step of 5 au and a fictitious electron mass of 400 au was employed. For the MM region, the leapfrog algorithm was used. The time step for integration was 1 fs and the cutoff for nonbond calculations was 1.0 nm. The total simulation time was 37.5 ps.

RESULTS/DISCUSSION

The second proton transfer undergoes different pathways in the five independent simulations. In Models A and B, the proton was delivered to the distal oxygen and led to the formation of Cpd I and a water molecule (coupling). Uncoupling was observed in Models C, D, and E. Both coupling and uncoupling were exothermic and finished rapidly during the simulation. Both reactions proceed without a barrier (or too small to be

dx.doi.org/10.1021/jp312107r | J. Phys. Chem. B XXXX, XXX, XXX−XXX

observed). It agrees with former studies, which show the second protonation is exothermic.[8,19,21,27] However, previous calculations provide very different results on the amount of energy released in the coupling reaction,[27,56] which is known to be due to the chosen model system and computational methodology.[24]

According to our calculations, coupling is thermodynamically more favorable than uncoupling by about 77 kcal/mol. However, among all of the five models, only two of them, A and B, lead to coupling. The other three, including C in which the hydroxyl group of the probe was equidistant to both O(p) and O(d), give uncoupling products. It suggests, for the peroxide atoms, that the results of competition for proton may depend on not only the differences in the electrostatic interaction between each oxygen atom and the to-be-transferred proton, but also the differences in the bond energy of O(p)-O(d) and Fe-O(p).

The Time-Dependent Bond Length and Bond Order Evolution. In chemical reactions, the progress of the reaction could be manifested by monitoring the dynamical changes of bond lengths and bond orders between reaction atoms. In this study, bond lengths of key atoms during the first 200 fs and the related Mayer bond orders during the reaction (50 fs) were captured (Figure 3). Evolutions of both parameters of Models A–E are shown in panels a–e, respectively (inset of each panel is for bond orders).

The changes of bond length and bond order of key bonds, e.g., H^+(aq)–O(d), H^+(aq)–O(p), and O(d)–O(p), in the reactions indicate that Models A and B are taking the coupling reaction, while Models C, D, and E undergoing uncoupling. In coupling cases (A and B), although the probe was at different distances and orientations to the hydroperoxo group, both exhibit a negative correlation between bond H^+(aq)–O(d) (decreasing) and O(d)–O(p) (increasing). The Pearson correlation coefficient is −0.93 in the case of A and −0.96 in B. The trajectories of these two reactions show that the approaching of H^+(aq) to O(d) and the stretching of bond O(d)–O(p) take place simultaneously. It is clear that the proton transfer and the O(d)–O(p) cleavage are coupled. This agrees well with former studies that the O(d)–O(p) cleavage is assisted by the second proton transfer.[8,23,28] Other studies that show O(d)–O(p) cleavage followed by proton transfer or proton transfer followed by O(d)–O(p) cleavage[23,24,30] may be due to the different proton sources and the different pathways.

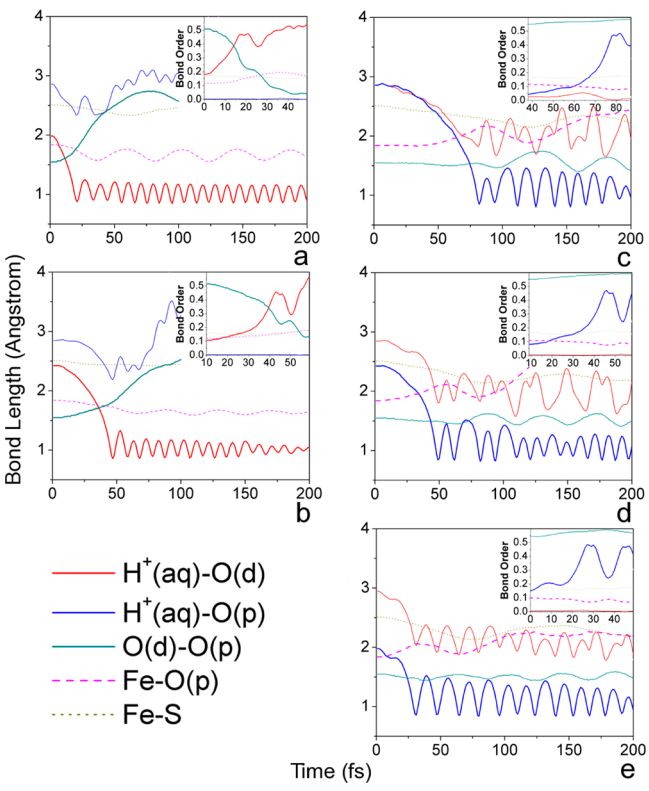

Figure 3. The time-dependent bond length and bond order evolution in simulations. In all reactions, the red, blue, and cyan curves represent the bond between proton of the probe [H^+(aq)] and the distal oxygen [O(d)] or the proximal oxygen [O(p)]. The dash line in pink is for the Fe–O(p) bond, while the dot line in dark green is for the Fe–S(Cys357) bond.

In uncoupling cases, the Fe–O(p) bond did not break immediately, but was weakened significantly. The lone pair electrons of one oxygen atom of H_2O_2 took up the unoccupied orbital of the iron atom. The formation of H^+(aq)–O(p) bond and the stretching of the Fe–O(p) bond also shows negative correlation. Coefficients of bond orders of these two bonds are −0.96, −0.99, and −0.99 for C, D, and E, respectively.

On the basis of the simulations, we are able to conclude that for both coupling and uncoupling, the proton transfer is associated with the O(d)–O(p) cleavage or the Fe–O(p) stretching.

Electronic Structure of the Reactions. Spin densities and natural charges of key atoms and groups were monitored to reveal the electronic structure change during the reactions. NBO population analysis[57] was performed at B3LYP/BS level (BS: LANL2DZ for Fe and 6-31G* for other atoms) with Gaussian09.[58] The spin densities and natural charges for Model A are shown in Figure 4a,b respectively, and those for Model E are shown in Figure 4c,d (for others, see Supporting Information). The spin densities and charges on the products Wat903 from coupling and H_2O_2 from uncoupling are the sum of leaving groups (OH^- + H^+ or OOH^- + H^+).

In view of population analysis, the negative charge on O(d) increases during the coupling process, which is accompanied by the decrease of the charge on porphyrin. Meanwhile, the spin density on O(d) does not change much, while that on O(p) and porphyrin increases. This suggests along with the proton transfer, that there is an electron transfer from porphyrin to the hydroperoxo unit to neutralize the positive charge of the incoming proton. A water molecule (Wat903) is produced after the heterolytic cleavage of the O(p)–O(d) bond. Thus, the proton transfer follows a proton-coupled electron transfer (PCET) mechanism.[24]

In the uncoupling reaction, spin density on the hydrogen peroxide diminishes during the reaction. The electron that is used to neutralize the charge on the proton probe comes from Fe and Cys ligand. Porphyrin does not contribute much to the electron transfer in uncoupling.

We note that the porphyrin ring plays different roles in coupling and uncoupling reactions. During coupling process, the heterolytic cleavage of the O(p)–O(d) bond gives a ferryl species with a high valent Fe atom, which is stabilized by the charge transfer from the porphyrin. In the uncoupling reaction, the Fe(III)–O(p) bond is broken, the enzyme goes back to its resting state and a molecule of hydrogen peroxide is generated. This does not require additional electrons to be pumped into the hydroperoxo unit, thus producing less influence on the

dx.doi.org/10.1021/jp312107r | J. Phys. Chem. B XXXX, XXX, XXX–XXX

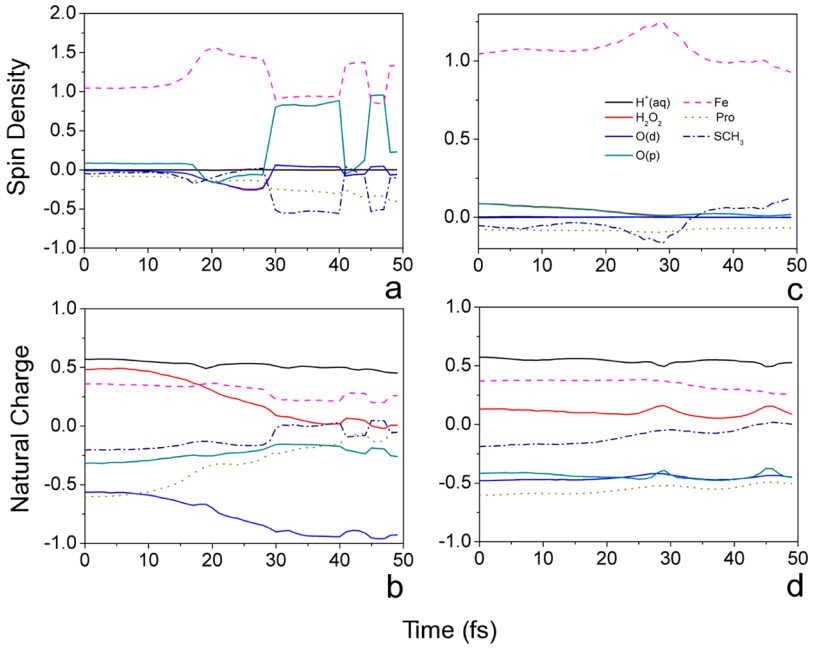

Figure 4. Spin densities (upper panels) and natural charges (lower panels) during the reactions of both coupling and uncoupling. Panels a and b are for Model A, showing the change of spin densities and natural charges, respectively. Panels c and d plot the change of spin densities and natural charges in Model E. The black, red, blue, and green lines represent the spin density/charge population on the proton, product (water or hydrogen peroxide), O(p), and O(d), respectively. The pink dash line is for the iron atom, the dark yellow dot line is for the porphyrin, while the ligand Cys is represented in navy.

electronic structure of the rest part of the molecule. These observations show that porphyrin can help to stabilize the ferryl species formed in the coupling process, but it does not have preference on either the coupling or the uncoupling reaction for the second proton transfer of P450cam. We have also observed the response of the proximal Cys ligand during the proton transfer. However, it is insufficient to distinguish its roles in the two reactions.

Discussion. In the present study, five models, A–E, representing possible pathways of the second proton transfer in different Thr252 mutants, were explored using the CPMD/MM dynamics simulation method. A previous QM/MM study[25] of Thiel and co-workers reported energy profiles for the second proton transfer in several P450cam mutants with Thr252 replaced by serine (T252S), valine (T252V), alanine (T252A), and glycine (T252G). They discussed the competition between the coupling (formation of Cpd I) and the uncoupling reactions (recovery of the ferric resting state) from the view of potential energies. However, in the present study, we aim to tackle the role of water molecules, which work as part of the hydrogen bond network in the vicinity of the ferric hydroperoxo moiety and then to elucidate the importance of the topology of water chains within the active site pocket. For this purpose, different models were built by placing a hydronium probe in the pocket according to the local topology of the wild-type P450cam and its T252X (X = S,V,A,G) mutants. These models make it possible for us to probe the dynamics of the second protonation at the last stage when the proton attaches to the FeOOH moiety, either to O(d) (coupling reaction) or to O(p) (uncoupling reaction). Based on the diverse propensities of the proton transfer to progress into either the coupling or the uncoupling reaction in the five models, we can unambiguously conclude that the local topology of the water chain is one of the determining factors on the fate of Cpd 0 upon the attachment of one proton.

According to our simulations, in coupling reaction, the O(d)–O(p) cleavage and the proton delivery are coupled with an electron transfer process. The protonated Cpd 0 (prot-Cpd 0: $FeOOH_2$) found by Zheng et al.[24] was not observed. This is conceivable concerning that prot-Cpd 0 is unstable and only found when the proton is transferred through the Glu366-Thr252 channel. In addition, the FeO···HO hydrogen-bonded intermediate (IC1 in their study) were not observed either. One possible reason is because IC1 is located in a small well on the potential energy surface; it is not difficult to overcome the low barrier (about 3 kcal/mol) in the dynamics simulation of an exothermic reaction. Moreover, as shown in Zheng et al.'s study,[24] the feature of the O(d)–O(p) cleavage strongly depends on the choice of QM region and moderately on the basis set. Without a sufficient theoretical treatment of the protein environment, the spin state of the forming OH species is a priori unknown whether it is a radical or an anion. Although the Cpd I in P450 has been captured for the first time[13] in a recent experiment, we do not know how the leaving OH group is consumed. It may undergo a heme degradation[59,60] like that in heme-oxygenase (HO), however, it is out of the scope of this article. We focus on the factor that determines the coupling/uncoupling reaction during the transition from Cpd 0 to Cpd I.

The presence of a proton in the vicinity of Thr252 is in reality feasible concerning the negative electronic potential of Cpd 0, which may drive the delivery of a proton from the bulk solvent to the active site. The energy cost is comparable in the five models we have investigated. Thus, in the current study, it is possible for us to focus on the proton transfer pathway which is determined by the hydrophobicity and volume of the side chain of residues in the active site to explore how it affects the selection between coupling and uncoupling.

Our study shows that the coupling process is associated with the proton delivery pathways represented in Models A and B, while the uncoupling is associated with those in Models C, D,

dx.doi.org/10.1021/jp312107r | J. Phys. Chem. B XXXX, XXX, XXX–XXX

and E. This suggests that the results of O(d) and O(p) competing for the proton depends on the delivery pathway of the proton to some extent, rather than fully on their proton affinity [The natural charge on O(d) is about −0.56e, while it is −0.32e on O(p)]. It shows the importance of the topology of active site, and is consistent with the previous mutagenesis study[61−65] and theoretical work[25] on the P450cam system. Thus, it is clear in the wild-type enzyme that the proton is delivered through the pathway in Model A, the Asp251-Thr252 channel, leading to a coupling process exclusively. When Thr252 is mutated to Ala or Gly, the channel is disrupted due to the absence of the terminal of a well-structured proton transfer network, which increases the probability of the proton undergoing other pathways, for example, pathways in Models C, D, and E, thus leads to uncoupling reactions.

CONCLUSIONS

We've carried out a series of CPMD/MM simulations to investigate the relevance of the second proton transfer pathway and the subsequent coupling/uncoupling reactions of P450cam. Five possible pathways were explored. Two of them (Models A and B) led to coupling reaction, while the other three (Models C−E) generated uncoupling products. During each reaction, bond properties between key atoms and electronic structure of the QM region were monitored. It shows that in the coupling reaction, O(d)−O(p) cleavage, proton transfer and electron delivery are coupled, while in the uncoupling reaction, stretching of the Fe−O(p) bond and proton transfer take place spontaneously. Moreover, the reactions of the second proton transfer (coupling or uncoupling) seem to be governed by the pathway the proton being delivered. The enzyme is likely to keep a high coupling rate by maintaining a specific proton transfer channel, the Asp251-Thr252 channel, through which the second proton is transferred to the ideal position for coupling reaction.

ASSOCIATED CONTENT

Supporting Information

The experimental data on coupling and uncoupling, the changes of spin densities, and natural charges and Mulliken charges in all of the five models are available free of charge via the Internet at http://pubs.acs.org.

AUTHOR INFORMATION

Corresponding Author

*Phone and fax: (86) 21-3420-4573. E-mail: dqwei@sjtu.edu.cn (D.-Q. Wei) or dwang@ihep.ac.cn (D.-Q. Wang).

Notes

The authors declare no competing financial interest.

ACKNOWLEDGMENTS

This work is supported by grants from the National High-Tech R&D Program (863 Program Contract No. 2012AA020307), the National Basic Research Program of China (973 Program) (Contract No. 2012CB721000), the Key Project of Shanghai Science and Technology Commission (Contract No. 11JC1406400), and Ph.D. Programs Foundation of Ministry of Education of China (Contract No. 20120073110057), which were awarded to D. Q. Wei.

REFERENCES

(1) Ortiz de Montellano, P. R., Ed. *Cytochrome P450: Structure, Mechanism, and Biochemistry*; Klewer Academic/Plenum Publishers: New York, 2005.

(2) Dawson, J. H.; Sono, M. Cytochrome P-450 and Chloroperoxidase: Thiolate-Ligated Heme Enzymes. Spectroscopic Determination of Their Active-Site Structures and Mechanistic Implications of Thiolate Ligation. *Chem. Rev.* **1987**, *87*, 1255−1276.

(3) Sono, M.; Roach, M. P.; Coulter, E. D.; Dawson, J. H. Heme-Containing Oxygenases. *Chem. Rev.* **1996**, *96*, 2841−2887.

(4) Hawkes, D. B.; Adams, G. W.; Burlingame, A. L.; Ortiz de Montellano, P. R.; De Voss, J. J. Cytochrome P450cin (CYP176A), Isolation, Expression, and Characterization. *J. Biol. Chem.* **2002**, *277*, 27725−27732.

(5) Denisov, I. G.; Makris, T. M.; Sligar, S. G.; Schlichting, I. Structure and Chemistry of Cytochrome P450. *Chem. Rev.* **2005**, *105*, 2253−2277.

(6) de Visser, S. P.; Valentine, J. S.; Nam, W. A Biomimetic Ferric Hydroperoxo Porphyrin Intermediate. *Angew. Chem., Int. Ed.* **2010**, *49*, 2099−2101.

(7) Coon, M. J. Cytochrome P450: Nature's Most Versatile Biological Catalyst. *Annu. Rev. Pharmacol. Toxicol.* **2005**, *45*, 1−25.

(8) Guallar, V.; Friesner, R. A. Cytochrome P450CAM Enzymatic Catalysis Cycle: A Quantum Mechanics/Molecular Mechanics Study. *J. Am. Chem. Soc.* **2004**, *126*, 8501−8508.

(9) Gunsalus, I. C.; Pederson, T. C.; Sligar, S. G. Oxygenase-Catalyzed Biological Hydroxylations. *Annu. Rev. Biochem.* **1975**, *44*, 377−407.

(10) Schlichting, I.; Berendzen, J.; Chu, K.; Stock, A. M.; Maves, S. A.; Benson, D. E.; Sweet, R. M.; Ringe, D.; Petsko, G. A.; Sligar, S. G. The Catalytic Pathway of Cytochrome P450cam at Atomic Resolution. *Science* **2000**, *287*, 1615−1622.

(11) Egawa, T.; Shimada, H.; Ishimura, Y. Evidence for Compound I Formation in the Reaction of Cytochrome-P450cam with M-Chloroperbenzoic Acid. *Biochem. Biophys. Res. Commun.* **1994**, *201*, 1464−1469.

(12) Kellner, D. G.; Hung, S. C.; Weiss, K. E.; Sligar, S. G. Kinetic Characterization of Compound I Formation in the Thermostable Cytochrome P450 CYP119. *J. Biol. Chem.* **2002**, *277*, 9641−9644.

(13) Rittle, J.; Green, M. T. Cytochrome P450 Compound I: Capture, Characterization, and CH Bond Activation Kinetics. *Science* **2010**, *330*, 933−937.

(14) Meunier, B.; de Visser, S. P.; Shaik, S. Mechanism of Oxidation Reactions Catalyzed by Cytochrome P450 Enzymes. *Chem. Rev.* **2004**, *104*, 3947−3980.

(15) Shaik, S.; Cohen, S.; Wang, Y.; Chen, H.; Kumar, D.; Thiel, W. P450 Enzymes: Their Structure, Reactivity, and Selectivity-Modeled by QM/MM Calculations. *Chem. Rev.* **2010**, *110*, 949−1017.

(16) Liu, J. G.; Ohta, T.; Yamaguchi, S.; Ogura, T.; Sakamoto, S.; Maeda, Y.; Naruta, Y. Spectroscopic Characterization of a Hydroperoxo-Heme Intermediate: Conversion of a Side-On Peroxo to an End-On Hydroperoxo Complex. *Angew. Chem., Int. Ed.* **2009**, *48*, 9262−9267.

(17) Newcomb, M.; Shen, R.; Choi, S. Y.; Toy, P. H.; Hollenberg, P. F.; Vaz, A. D. N.; Coon, M. J. Cytochrome P450-Catalyzed Hydroxylation of Mechanistic Probes that Distinguish between Radicals and Cations. Evidence for Cationic but Not for Radical Intermediates. *J. Am. Chem. Soc.* **2000**, *122*, 2677−2686.

(18) Vaz, A. D. N.; McGinnity, D. F.; Coon, M. J. Epoxidation of Olefins by Cytochrome P450: Evidence from Site-Specific Mutagenesis for Hydroperoxo-Iron as an Electrophilic Oxidant. *Proc. Natl. Acad. Sci. U.S.A.* **1998**, *95*, 3555−3560.

(19) Ogliaro, F.; de Visser, S. P.; Cohen, S.; Sharma, P. K.; Shaik, S. Searching for the Second Oxidant in the Catalytic Cycle of Cytochrome P450: A Theoretical Investigation of the Iron (III)-Hydroperoxo Species and Its Epoxidation Pathways. *J. Am. Chem. Soc.* **2002**, *124*, 2806−2817.

(20) Shaik, S.; de Visser, S. P.; Ogliaro, F.; Schwarz, H.; Schroder, D. Two-State Reactivity Mechanisms of Hydroxylation and Epoxidation

by Cytochrome P-450 Revealed by Theory. *Curr. Opin. Chem. Biol.* **2002**, *6*, 556−567.
(21) Kamachi, T.; Shiota, Y.; Ohta, T.; Yoshizawa, K. Does the Hydroperoxo Species of Cytochrome P450 Participate in Olefin Epoxidation with the Main Oxidant, Compound I? Criticism from Density Functional Theory Calculations. *Bull. Chem. Soc. Jpn.* **2003**, *76*, 721−732.
(22) Park, M. J.; Lee, J.; Suh, Y.; Kim, J.; Nam, W. Reactivities of Mononuclear Non-Heme Iron Intermediates including Evidence that Iron(III)−Hydroperoxo Species is a Sluggish Oxidant. *J. Am. Chem. Soc.* **2006**, *128*, 2630−2634.
(23) Kumar, D.; Hirao, H.; de Visser, S. P.; Zheng, J. J.; Wang, D. Q.; Thiel, W.; Shaik, S. New Features in the Catalytic Cycle of Cytochrome P450 during the Formation of Compound I from Compound 0. *J. Phys. Chem. B* **2005**, *109*, 19946−19951.
(24) Zheng, J. J.; Wang, D. Q.; Thiel, W.; Shaik, S. QM/MM Study of Mechanisms for Compound I Formation in the Catalytic Cycle of Cytochrome P450cam. *J. Am. Chem. Soc.* **2006**, *128*, 13204−13215.
(25) Altarsha, M.; Benighaus, T.; Kumar, D.; Thiel, W. How is the Reactivity of Cytochrome P450cam Affected by Thr252X Mutation? A QM/MM Study for X = Serine, Valine, Alanine, Glycine. *J. Am. Chem. Soc.* **2009**, *131*, 4755−4763.
(26) Altarsha, M.; Wang, D.; Benighaus, T.; Kumar, D.; Thiel, W. QM/MM Study of the Second Proton Transfer in the Catalytic Cycle of the D251N Mutant of Cytochrome P450cam. *J. Phys. Chem. B* **2009**, *113*, 9577−9588.
(27) Harris, D. L.; Loew, G. H. Theoretical Investigation of the Proton Assisted Pathway to Formation of Cytochrome P450 Compound I. *J. Am. Chem. Soc.* **1998**, *120*, 8941−8948.
(28) Hata, M.; Hirano, Y.; Hoshino, T.; Nishida, R.; Tsuda, M. Theoretical Study on Compound I Formation in Monooxygenation Mechanism by Cytochrome P450. *J. Phys. Chem. B* **2004**, *108*, 11189−11195.
(29) Shaik, S.; Kumar, D.; de Visser, S. P.; Altun, A.; Thiel, W. Theoretical Perspective on the Structure and Mechanism of Cytochrome P450 Enzymes. *Chem. Rev.* **2005**, *105*, 2279−2328.
(30) Sen, K.; Hackett, J. C. Molecular Oxygen Activation and Proton Transfer Mechanisms in Lanosterol 14a-Demethylase Catalysis. *J. Phys. Chem. B* **2009**, *113*, 8170−8182.
(31) Altarsha, M.; Benighaus, T.; Kumar, D.; Thiel, W. Coupling and Uncoupling Mechanisms in the Methoxythreonine Mutant of Cytochrome P450cam: A Quantum Mechanical/Molecular Mechanical Study. *J. Biol. Inorg. Chem.* **2010**, *15*, 361−372.
(32) Taraphder, S.; Hummer, G. Protein Side-Chain Motion and Hydration in Proton-Transfer Pathways. Results for Cytochrome P450cam. *J. Am. Chem. Soc.* **2003**, *125*, 3931−3940.
(33) Vidakovic, M.; Sligar, S.; Li, H.; Poulos, T. Understanding the Role of the Essential Asp251 in Cytochrome P450cam Using Site-Directed Mutagenesis, Crystallography, and Kinetic Solvent Isotope Effect. *Biochemistry* **1998**, *37*, 9211−9219.
(34) Agmon, N. The Grotthuss Mechanism. *Chem. Phys. Lett.* **1995**, *244*, 456−462.
(35) Schoneboom, J. C.; Lin, H.; Reuter, N.; Thiel, W.; Cohen, S.; Ogliaro, F.; Shaik, S. The Elusive Oxidant Species of Cytochrome P450 Enzymes: Characterization by Combined Quantum Mechanical/Molecular Mechanical (QM/MM) Calculations. *J. Am. Chem. Soc.* **2002**, *124*, 8142−8151.
(36) Schoneboom, J. C.; Thiel, W. The Resting State of P450cam: A QM/MM Study. *J. Phys. Chem. B* **2004**, *108*, 7468−7478.
(37) Altun, A.; Thiel, W. Combined Quantum Mechanical/Molecular Mechanical Study on the Pentacoordinated Ferric and Ferrous Cytochrome P450cam Complexes. *J. Phys. Chem. B* **2005**, *109*, 1268−1280.
(38) Wang, D.; Zheng, J.; Shaik, S.; Thiel, W. Quantum and Molecular Mechanical Study of the First Proton Transfer in the Catalytic Cycle of Cytochrome P450cam and Its Mutant D251N. *J. Phys. Chem. B* **2008**, *112*, 5126−5138.
(39) Koster, A. M.; Flores-Moreno, R.; Geudtner, G.; Goursot, A.; Heine, T.; Reveles, J. U.; Vela, A.; Salahub, D. R. *deMon 2003 Code*; NRC: Ottawa, Canada, 2003.
(40) Berendsen, H. J. C.; Postma, J. P. M.; van Gunsteren, W. F.; Hermans, J. Interaction Models for Water in Relation to Protein Hydration. In *Intermolecular Forces*; Pullman, B., Ed.; D. Reidel Publishing Company: Dordrecht, The Netherlands, 1981; pp 331−342.
(41) Oprea, T. I.; Hummer, G.; García, A. E. Identification of a Functional Water Channel in Cytochrome P450 Enzymes. *Proc. Natl. Acad. Sci. U.S.A.* **1997**, *94*, 2133−2138.
(42) Becke, A. D. Density-Functional Exchange-Energy Approximation with Correct Asymptotic Behavior. *Phys. Rev. A* **1988**, *38*, 3098−3100.
(43) Vanderbilt, D. Soft Self-Consistent Pseudopotentials in a Generalized Eigenvalue Formalism. *Phys. Rev. B* **1990**, *41*, 7892−7895.
(44) Laasonen, K.; Car, R.; Lee, C.; Vanderbilt, D. Implementation of Ultrasoft Pseudopotentials in *Ab Initio* Molecular Dynamics. *Phys. Rev. B* **1991**, *43*, 6796−6799.
(45) Laasonen, K.; Pasquarello, A.; Car, R.; Lee, C.; Vanderbilt, D. Car−Parrinello Molecular Dynamics with Vanderbilt Ultrasoft Pseudopotentials. *Phys. Rev. B* **1993**, *47*, 10142−10153.
(46) Jorgensen, W. L.; Tirado-Rives, J. The OPLS Force Field for Proteins. Energy Minimizations for Crystals of Cyclic Peptides and Crambin. *J. Am. Chem. Soc.* **1988**, *110*, 1657−1666.
(47) Jorgensen, W. L.; Maxwell, D. S.; Tirado-Rives, J. Development and Testing of the OPLS All-Atom Force Field on Conformational Energetics and Properties of Organic Liquids. *J. Am. Chem. Soc.* **1996**, *118*, 11225−11236.
(48) Berendsen, H. J. C.; van der Spoel, D.; van Drunen, R. GROMACS: A Message-Passing Parallel Molecular Dynamics Implementation. *Comput. Phys. Commun.* **1995**, *91*, 43−56.
(49) Lindahl, E.; Hess, B.; van der Spoel, D. GROMACS 3.0: A Package for Molecular Simulation and Trajectory Analysis. *J. Mol. Model.* **2001**, *7*, 306−317.
(50) van der Spoel, D.; Lindahl, E.; Hess, B.; Groenhof, G.; Mark, A. E.; Berendsen, H. J. C. GROMACS: Fast, Flexible, and Free. *J. Comput. Chem.* **2005**, *26*, 1701−1718.
(51) Biswas, P. K.; Gogonea, V. A Regularized and Renormalized Electrostatic Coupling Hamiltonian for Hybrid Quantum-Mechanical-Molecular-Mechanical Calculations. *J. Chem. Phys.* **2005**, *123*, 164114−164122.
(52) Das, D.; Eurenius, K. P.; Billings, E. M.; Sherwood, P.; Chatfield, D. C.; Hodoscek, M.; Brooks, B. R. Optimization of Quantum Mechanical Molecular Mechanical Partitioning Schemes: Gaussian Delocalization of Molecular Mechanical Charges and the Double Link Atom Method. *J. Chem. Phys.* **2002**, *117*, 10534−10547.
(53) Hestenes, M. R.; Stiefel, E. Methods of Conjugate Gradients for Solving Linear Systems. *J. Res. Natl. Bur. Stand.* **1952**, *49*, 409−436.
(54) Berendsen, H. J. C.; Postma, J. P. M.; Vangunsteren, W. F.; Dinola, A.; Haak, J. R. Molecular-Dynamics with Coupling to an External Bath. *J. Chem. Phys.* **1984**, *81*, 3684−3690.
(55) Car, R.; Parrinello, M. Unified Approach for Molecular-Dynamics and Density-Functional Theory. *Phys. Rev. Lett.* **1985**, *55*, 2471−2474.
(56) Kamachi, T.; Yoshizawa, K. A Theoretical Study on the Mechanism of Camphor Hydroxylation by Compound I of Cytochrome P450. *J. Am. Chem. Soc.* **2003**, *125*, 4652−4661.
(57) Glendening, E. D.; Reed, A. E.; Carpenter, J. E.; Weinhold, F. *NBO Version 3.1*.
(58) Frisch, M. J.; Trucks, G. W.; Schlegel, H. B.; Scuseria, G. E.; Robb, M. A.; Cheeseman, J. R.; Scalmani, G.; Barone, V.; Mennucci, B.; Petersson, G. A.; et al. *Gaussian 09*, revision A.1; Gaussian, Inc.: Wallingford CT, 2009.
(59) Sharma, P. K.; Kevorkiants, R.; de Visser, S. P.; Kumar, D.; Shaik, S. Porphyrin Traps Its Terminator! Concerted and Stepwise Porphyrin Degradation Mechanisms Induced by Heme-Oxygenase and Cytochrome P450. *Angew. Chem.* **2004**, *116*, 1149−1152.

(60) Derat, E.; Kumar, D.; Hirao, H.; Shaik, S. Gauging the Relative Oxidative Powers of Compound I, Ferric-Hydroperoxide, and the Ferric-Hydrogen Peroxide Species of Cytochrome P450 toward CH Hydroxylation of a Radical Clock Substrate. *J. Am. Chem. Soc.* **2006**, *128*, 473−484.
(61) Shimada, H.; Makino, R.; Imai, M.; Horiuchi, T.; Ishimura, Y. Mechanism of Oxygen Activation by Cytochrome P-450cam. *International Symposium on Oxygenases and Oxygen Activation: Yamada Conference XXVII*, 1990, Osaka, Japan.
(62) Gerber, N. C.; Sligar, S. G. Catalytic Mechanism of Cytochrome P-450: Evidence for a Distal Charge Relay. *J. Am. Chem. Soc.* **1992**, *114*, 8742−8743.
(63) Hishik, T.; Shimada, H.; Nagano, S.; Egawa, T.; Kanamori, Y.; Makino, R.; Park, S. Y.; Adachi, S.; Shiro, Y.; Ishimura, Y. X-ray Crystal Structure and Catalytic Properties of Thr252Ile Mutant of Cytochrome P450cam: Roles of Thr252 and Water in the Active Center. *J. Biochem.* **2000**, *128*, 965−974.
(64) Imai, M.; Shimada, H.; Watanabe, Y.; Matsushima-Hibiya, Y.; Makino, R.; Koga, H.; Horiuchi, T.; Ishimura, Y. Uncoupling of the Cytochrome P-450cam Monooxygenase Reaction by a Single Mutation, Threonine-252 to Alanine or Valine: Possible Role of the Hydroxy Amino Acid in Oxygen Activation. *Proc. Natl. Acad. Sci. U.S.A.* **1989**, *86*, 7823−7827.
(65) Kimata, Y.; Shimada, H.; Hirose, T.; Ishimura, Y. Role of Thr-252 in Cytochrome P450(Cam): A Study with Unnatural Amino-Acid Mutagenesis. *Biochem. Biophys. Res. Commun.* **1995**, *208*, 96−102.